

Controlled Chemical and Structural Properties of Mixed Self-Assembled Monolayers by Coadsorption of Symmetric and Asymmetric Disulfides on Au(111)

Shengfu Chen, Lingyan Li, Christina L. Boozer, and Shaoyi Jiang*

Department of Chemical Engineering, University of Washington, Box 351750, Seattle, Washington 98195-1750

Received: November 8, 2000; In Final Form: February 5, 2001

We present a new method of controlling nanoscale structures of mixed self-assembled monolayers (SAMs) on atomically flat Au(111) surfaces by coadsorption from a solution containing asymmetric and symmetric disulfides. Our results showed that the mixed disulfides formed homogeneous SAMs, whereas the mixed thiols with similar surface compositions led to phase segregation on the Au(111) surfaces. The disulfides were chosen so as to produce the same surface thiolates as the thiols. Nanoscale phase segregated domains were characterized and identified by atomic force/friction force microscopy (AFM/FFM). Preferential adsorption of the mixed SAMs was determined by X-ray photoelectron spectroscopy (XPS). There was less preferential adsorption and phase segregation of the mixed SAMs prepared by disulfides than thiols. The possible mechanism of the formation of the uniform mixed SAMs by coadsorption of symmetric and asymmetric disulfides is discussed.

Introduction

The fabrication of nanoscale structures using self-assembled monolayers (SAMs) has recently attracted much attention due to its scientific importance and potential applications to chemical sensors, biosensors, and biocompatible materials.¹ Pure SAMs of thiols with different chain lengths and terminal groups on gold surfaces have been studied extensively.^{1,2} However, the SAMs of pure thiols have several problems, such as high densities of surface functional groups leading to steric hindrances,³ and less ordered structures due to bulky terminal groups used. Mixed SAMs are promising due to the possibility to control chemical and structural properties of a surface by adjusting the abundance, type, and spatial (both normal and lateral) distribution of tail groups.⁴ Several studies have shown that mixed SAMs can promote protein adsorption possibly due to multiple chemical functionalities on surfaces and decreased steric effects.⁵ The first three factors (i.e., abundance, type, and normal distribution) can be controlled by varying solution composition, terminal group, and chain length, respectively. The choice of these three factors depends on the particular application. The control of the fourth factor (i.e., lateral distribution) is somewhat more difficult. In many applications, it is desirable to create homogeneous mixed SAMs. Several methods were introduced to prepare mixed SAMs, including coadsorption of mixed thiols,⁹ insertion of a second component into incomplete SAMs,¹⁰ combination of LB and SAMs preparation,¹¹ and chemical modification of terminal groups.¹² However, the preparation of uniform mixed SAMs still presents many challenges because coadsorption from a solution containing two components will lead to phase segregation if these two components are quite different, for example, in chain length.⁶ Differences in dipoles⁷ or incompatible lattice constants could also lead to phase segregation. Therefore, it is important to elucidate the fundamental principles of the phase behavior of two-component monolayers on an atomically flat surface before it is possible to control surface properties for a specific

application.⁸ Recently, we developed a kinetically trapped method¹³ to prepare truly molecular-scale mixed SAMs. By simply increasing solution temperature, SAM defects decreased and the closely packed homogeneous mixed SAMs formed. The mixed SAMs were fully characterized by scanning tunneling (STM), atomic force (AFM), and friction force (FFM) microscopy.

In this work, we propose another new method for forming uniform mixed SAMs by coadsorption of asymmetrical and symmetrical disulfides. No systematic studies have been carried out to prepare uniform mixed SAMs with a variety of surface compositions using mixed disulfides so far. Recent reports on deviation from 1:1 composition in SAMs formed from adsorption of asymmetric disulfide on polycrystalline gold¹⁴ and dissociative adsorption of asymmetric disulfide¹⁵ make this approach questionable. Thermodynamically, the order of the stability of alkyl chain pairs in the SAMs is long chain–long chain > short chain–short chain > long chain–short chain.¹⁶ On the basis of this principle, we expect that for SAMs produced using mixed symmetric and asymmetric disulfides on atomically flat gold, less phase segregation and preferential adsorption will occur. This is because each long chain moiety will bring in a short chain due to the structure of the asymmetric disulfide when the disulfides adsorb. The short chains around a long chain block further aggregation of long chains. This hypothesis is illustrated in Figure 1.

To provide direct comparison of coadsorption results from thiols and disulfides, both thiols and disulfides were chosen so as to produce the same surface thiolates. Thus, mixed octadecanethiol [$\text{CH}_3(\text{CH}_2)_{17}\text{SH}$] and 11-mercaptoundecanol [$\text{HOCH}_2(\text{CH}_2)_{10}\text{SH}$], and mixed dioctadecyl 11-hydroxyundecyl disulfide [$\text{CH}_3(\text{CH}_2)_{17}\text{S}-\text{S}(\text{CH}_2)_{10}\text{CH}_2\text{OH}$] and di-11-hydroxyundecyl disulfide [$\text{HOCH}_2(\text{CH}_2)_{10}\text{S}-\text{S}(\text{CH}_2)_{10}\text{CH}_2\text{OH}$] were used in this study. The hydroxymethyl ($-\text{CH}_2\text{OH}$) group was chosen because it is relatively small and does not alter the lattice structure of methyl terminated alkanethiols. The $-\text{OH}$ terminal group was also chosen to allow the determination of the surface compositions of SAMs by X-ray photoelectron spectroscopy

* To whom correspondence should be addressed.

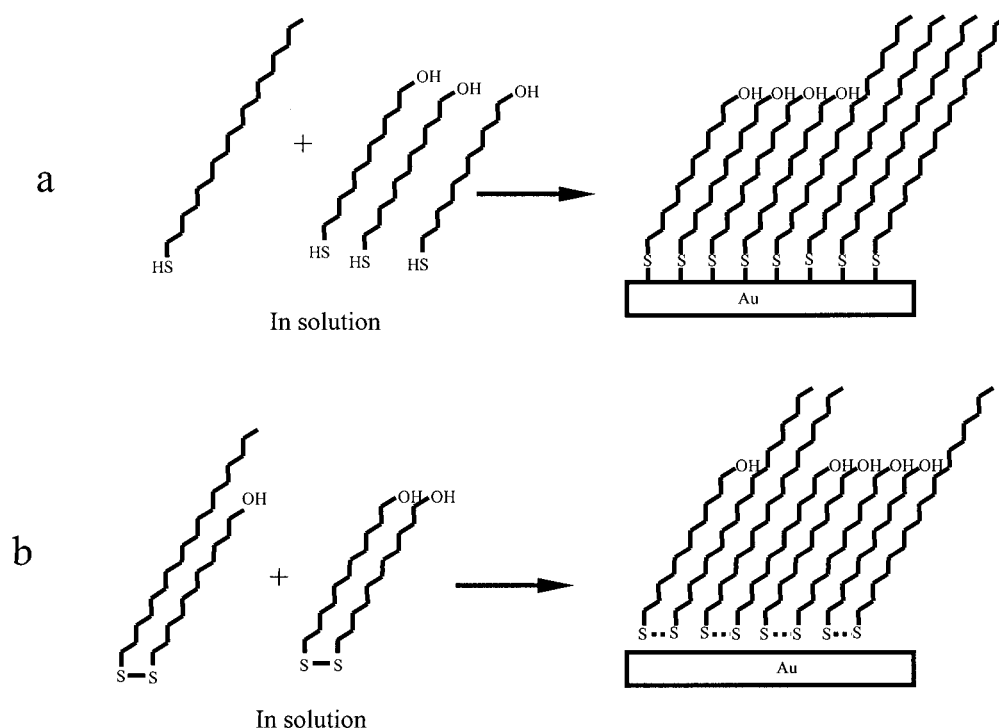


Figure 1. Illustration of the different mechanisms of the coadsorption from a solution containing mixed thiols (a) or disulfides (b), corresponding to phase segregation (a) or uniform phase (b), respectively. The dash line between two sulfur atoms in (b) represents the two chains belong to the same disulfide molecule in solution.

(XPS). Furthermore, this is a simple model surface with hydrophobic groups protruded out of a hydrophilic background potentially useful for future applications. AFM and FFM have been used to characterize nanoscale phase segregation and molecular-scale packing structure.¹⁷ To identify the existence of nanoscale domains, we examined each surface from $2 \times 2 \mu\text{m}^2$ down to $50 \times 50 \text{ nm}^2$ in this work by both AFM and FFM techniques.

Experimental Section

A. Chemical Synthesis. Octadecyl 11-hydroxyundecyl disulfide was prepared by the hydrolysis of Bunte salts, as developed by Milligan and Swan.¹⁸ A total of 6.2 g (81 mmol) of thiourea were dissolved in 25 mL of HCl (1 M). The solution was subsequently degassed for 20 min with nitrogen. A total of 2.3 g (8.15 mmol) of 1-octadecanethiol (Aldrich) were added and the solution was heated to reflux. A total of 2.5 g (8.15 mmol) of sodium 11-hydroxyundecyl thiosulfate (Bunte salt) dissolved in 25 mL of ethanol were added through a funnel. After 1 h of reflux, a kind of oil formed on the top of the reaction solution, which crystallizes upon cooling. The crude product was filtered, washed by water, and purified by flash chromatography on silica using chloroform as eluent. The fractions of asymmetric disulfide were dried at low pressure and recrystallized from acetone and ethanol. Yield: $\sim 300 \text{ mg}$. ^1H NMR (CDCl_3 , 200 MHz) δ (ppm): 0.86 (t, 3H, CH_3), 1.2–1.7 (m, 50H, CH_2 aliphatic), 2.66 (t, 4H, $\text{CH}_2\text{-S}$), and 3.62 (t, 2H, $\text{CH}_2\text{-O}$).

Di-11-hydroxyundecyl disulfide was also prepared by the hydrolysis of Bunte salts. A total of 1.2 g of 11-mercaptoundecanol Bunte salts and 0.22 g of 4-(dimethyl amino)-pyridine (DMAP) were dissolved in 17 mL of 1 M HCl. The solution was stirred for 1 h at 100°C . After cooling to room temperature, the disulfide precipitated and was filtered from the solvent. The product was re-crystallized from acetone and eth-

anol. Yield: $\sim 300 \text{ mg}$. ^1H NMR (CDCl_3 , 200 MHz) δ (ppm): 1.2–1.7 (m, 36H, CH_2 aliphatic), 2.66 (t, 4H, $\text{CH}_2\text{-S}$), 3.62 (t, 4H, $\text{CH}_2\text{-O}$).

B. Au(111) Preparation. Gold (Alfa Aesar, Ward Hill, MA, 99.9985%) was deposited onto freshly cleaved mica substrates (Mica New York Corp., clear ruby muscovite) in a high vacuum evaporator (BOC Edwards Auto306) at $\sim 10^{-7}$ Torr. Before deposition, mica was preheated to 325°C for 2 h by a radiator heater located behind the mica substrate to enhance the formation of large Au(111) terraces. The typical evaporation rate was 0.3 nm/s , and the thickness of gold films ranged from 150 to 200 nm. This method produced flat Au(111) terraces as large as $300 \text{ nm} \times 300 \text{ nm}$ according to our AFM measurements.

C. SAM Preparation. Octadecanethiol and 11-mercaptoundecanol were obtained from Aldrich Chemical Co. and were used as received. SAMs were formed by soaking gold-coated substrates (immediately after vacuum deposition or annealing by H_2 flame) in dilute ($\sim 1 \text{ mM}$) mixed thiol or disulfide solutions at room temperature. The substrates remained in the solutions for ~ 1 day. Prior to imaging, all of the SAMs were rinsed extensively with ethanol and dried under a stream of N_2 .

D. Atomic Force Microscopy (AFM). All AFM/FFM images were acquired with a Digital Instruments (DI) Multimode Nanoscope E (Santa Barbara, CA). The instrument is equipped with an E scanner (DI) and operated in air. For contact-mode AFM/FFM, a commercial Si_3N_4 cantilever of a nominal spring constant of 0.12 N/m from DI was used. The external force used for imaging was smaller than 5 nN . The relative humidity was less than 35%.

E. X-ray Photoelectron Spectroscopy (XPS). XPS spectra were obtained on a Surface Science Instruments (SSI) S-Probe ESCA using a $1000 \mu\text{m}$ spot size. An aluminum $\text{K}\alpha$ 1,2 monochromatized X-ray source (1486.6 eV) was used to stimulate photoemission. The energy of the emitted electrons

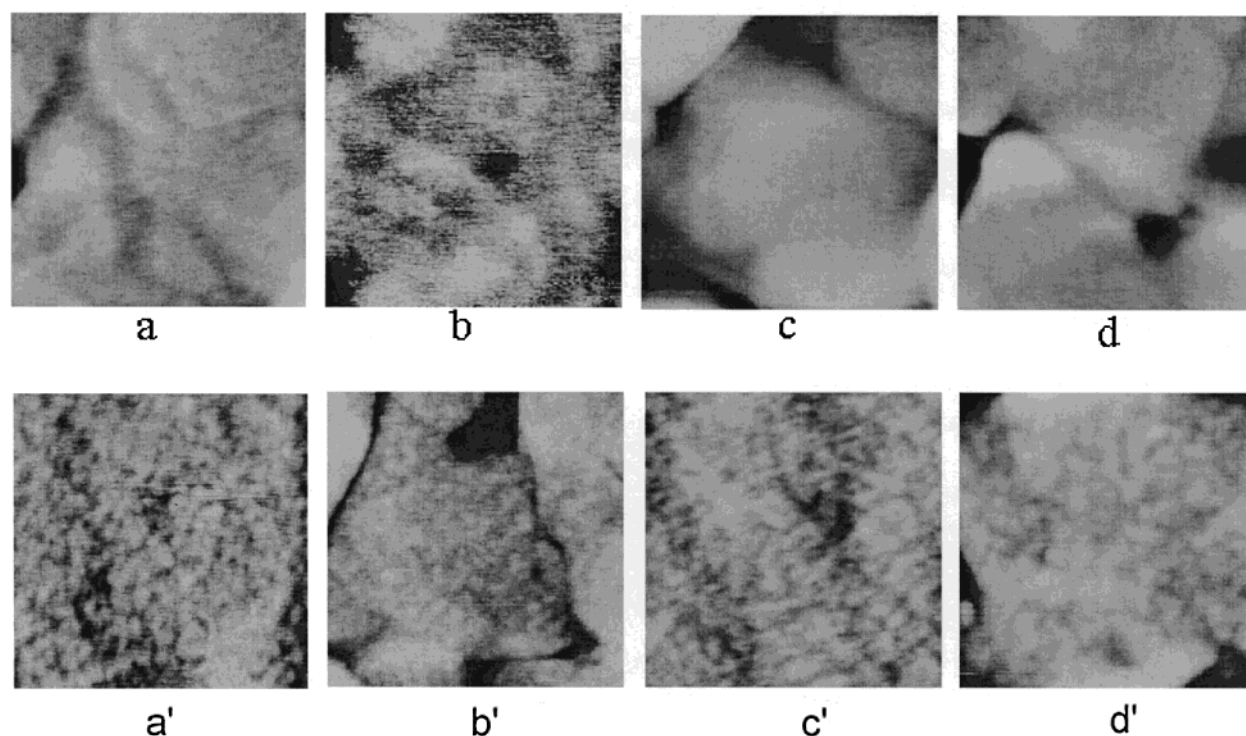


Figure 2. AFM images of the mixed SAMs formed by coadsorption of $\text{CH}_3(\text{CH}_2)_{17}\text{SH}$ and $\text{HOCH}_2(\text{CH}_2)_{10}\text{SH}$ immediately after the samples were brought out of the solutions (a–d) and kept in air for 3 days (a'–d'). The solution mol fraction of short chain is 0.80 (a and a'), 0.86 (b and b'), 0.89 (c and c'), and 0.92 (d and d'). Obvious phase segregation was observed in (a'–d'). The dimensions of the images are 500 nm \times 500 nm and the z range is 3 nm.

was measured with a hemispherical energy analyzer at the pass energy of 150 eV. Spectra were collected with the analyzer at 55° with respect to the surface normal of the sample. Typical pressures in the analysis chamber during spectral acquisition were 10^{-9} Torr. SSI data analysis software was used to calculate elemental compositions from the peak areas. The surface composition (molar fraction) of short chains [$\text{HOCH}_2(\text{CH}_2)_{10}\text{S}-$] was determined from XPS by scaling the O (1 s) signal of the mixed SAMs to that of pure $\text{HOCH}_2(\text{CH}_2)_{10}\text{SH}$ SAMs or $\text{HOCH}_2-(\text{CH}_2)_{10}\text{S}-\text{S}(\text{CH}_2)_{10}\text{CH}_2\text{OH}$.

Results and Discussion

1. Phase Segregated Mixed Thiols. AFM images in Figure 2 show the coadsorption results of $\text{HOCH}_2(\text{CH}_2)_{10}\text{SH}$ and $\text{CH}_3(\text{CH}_2)_{17}\text{SH}$ obtained immediately after the samples were brought out of the solutions (a–d) and were kept in air for 3 days (a'–d'). The surface compositions of short chains on these samples range from 0.22 to 0.77 determined by XPS, while the corresponding solution compositions of short chain range from 0.80 to 0.92. Phase segregation was not readily detected by AFM due to less ordered structures when the samples were just brought out of the solutions (Figure 2, a–d), whereas phase segregation became very clear due to recrystallization when they were kept in air for 3 days (Figure 2, a'–d'). Figure 3 shows an enlarged topographic image of Figure 1b' prepared from the solution with 0.86 short chain along with the corresponding frictional image. The approximate 2.5-fold difference in frictional coefficients between short chain [$\text{HOCH}_2(\text{CH}_2)_{10}\text{S}-$] and long chain [$\text{CH}_3(\text{CH}_2)_{17}\text{S}-$] monolayers in this system¹⁹ ensures a sufficient image contrast to identify domains of the different components. In Figure 3, the white domains in the topographic image are long chain rich phase. Their corresponding black spots in the frictional image show relatively lower friction. On the

basis of this relationship between the topographic and the frictional image, it is easy to identify phase segregation.

According to the thermodynamic principle, the order of stability of pairs of alkyl groups in the mixed SAMs is long chain–long chain > short chain–short chain > long chain–short chain.¹⁶ Because of the large energy difference between short and long chain pairs, their mixtures should segregate into one long chain rich and the other short chain rich phase. The SAM formation process on Au(111) is very complicated and the process usually consists of many steps,²⁰ such as chain exchange between solution and surface²¹ and change of chain conformation to a densely well packed 2-D crystal structure.²² The latter could be a rate-determining step. Our XPS results (given in the next section) showed that significant preferential adsorption occurred when the samples were just brought out of solution. This indicates that phase segregation occurs in solution as a result of chain exchange between solution and surface. For the samples just brought out of solution, the alkyl chains of the mixed SAMs on the surface were still less ordered, leading to a low contrast in AFM/FFM image as observed in Figure 2 (panels a–d). As time passes, chain conformations change to crystalline states. Such conformation change occurs locally. The possibility for thiols to move around freely on the surface is very low due to the relatively compact structure of SAMs.¹³ It has been found in this work along with previous reports^{23,24} that mixed SAMs formed by thiols and disulfides are the same except that the coverage of disulfide SAMs is lower than that of thiol SAMs. The absence of phase segregation for the lower-coverage disulfides as shown below further support the observation that thiols cannot move freely on the surface in the mixed thiol SAMs. As a result, phase segregation of the mixed SAMs kept in air for 3 days is readily observed by AFM as shown in Figure 2 (panels a'–d'). Phase segregated SAMs formed from mixed thiols are not desirable for many applications. For

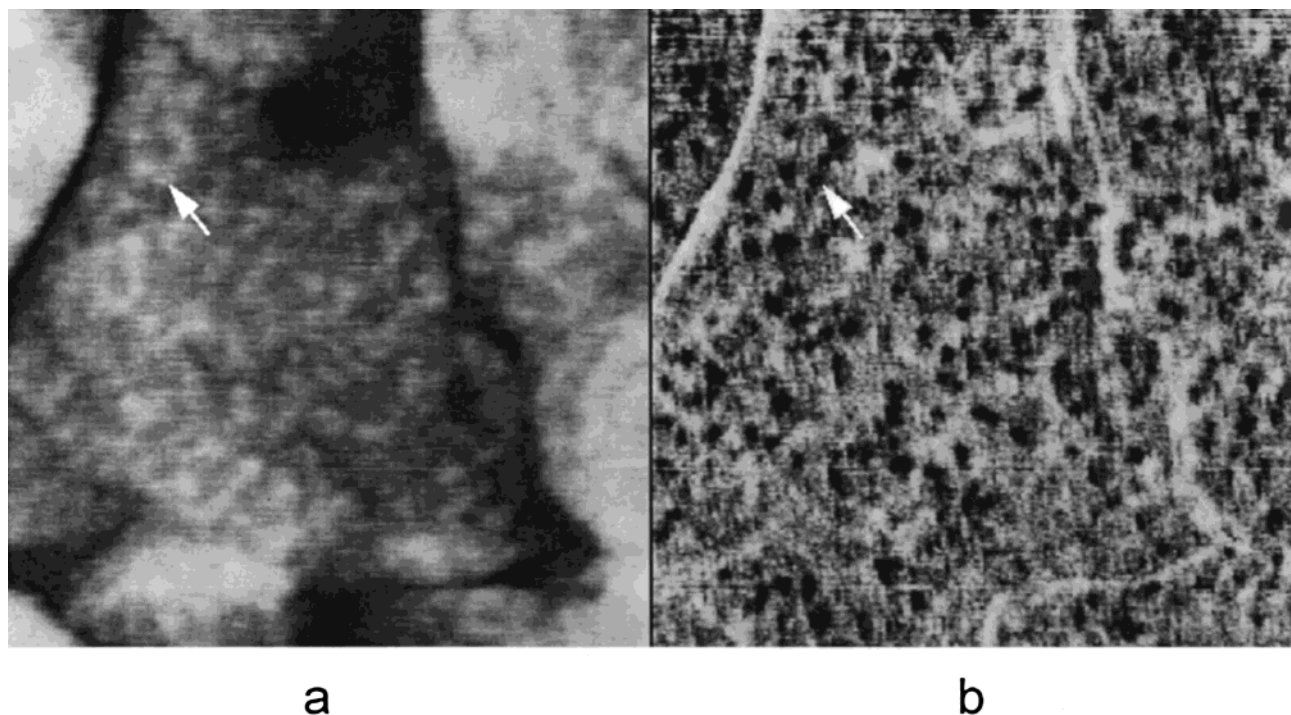


Figure 3. Enlarged AFM (a) and FFM (b) images of the mixed SAMs of $\text{CH}_3(\text{CH}_2)_{17}\text{SH}$ and $\text{HOCH}_2(\text{CH}_2)_{10}\text{SH}$ of Figure 1b'. There exists obvious phase segregation. The white domains in the height image are $\text{CH}_3(\text{CH}_2)_{17}\text{SH}$ rich phase. Their corresponding black spots in the frictional image show relatively low friction. The dimensions of the images are 500 nm \times 500 nm. The z ranges are 3 nm (a) and 0.05 v (b).

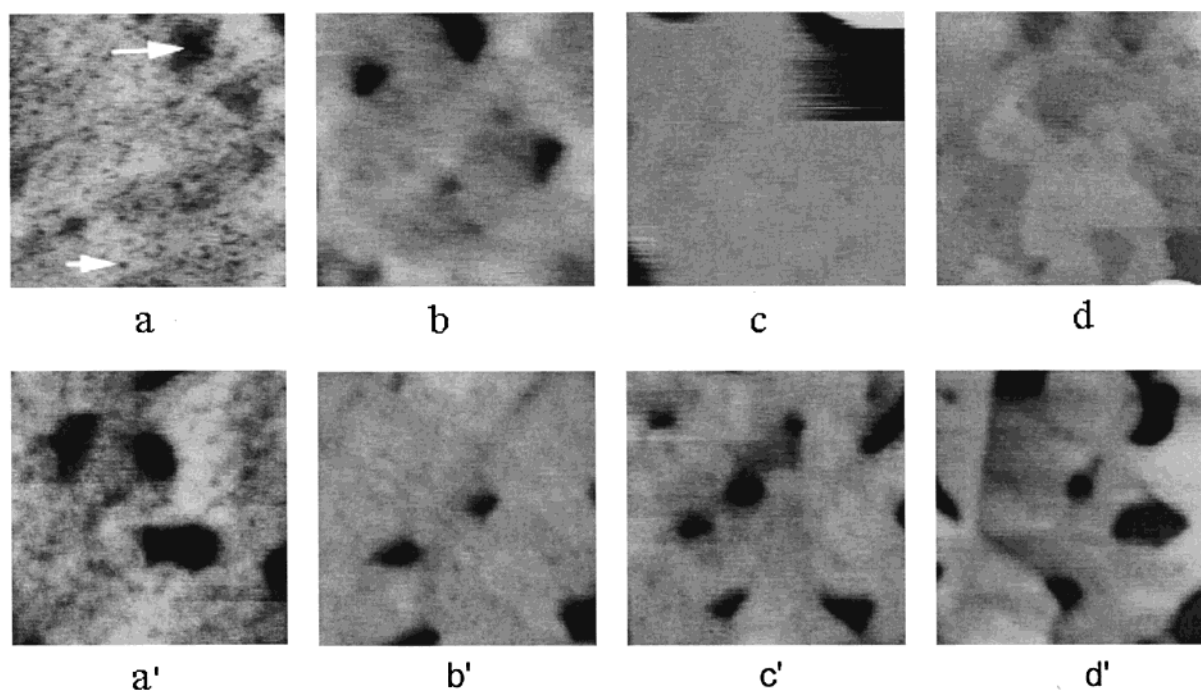


Figure 4. AFM images of the mixed SAMs formed by coadsorption of $\text{CH}_3(\text{CH}_2)_{17}\text{S}-\text{S}(\text{CH}_2)_{10}\text{CH}_2\text{OH}$ and $\text{HOCH}_2(\text{CH}_2)_{10}\text{S}-\text{S}(\text{CH}_2)_{10}\text{CH}_2\text{OH}$ immediately after the samples were brought out of the solutions (a–d) and 3 days later (a'–d'). The solution mol fraction of $\text{HOCH}_2(\text{CH}_2)_{10}\text{S}$ -chain is 0.50 (a and a'), 0.75 (b and b'), 0.83 (c and c'), and 0.90 (d and d'). No obvious phase segregation was found for all cases. The smaller and larger holes marked in panel a are SAM defects and gold pits, respectively. The dimensions of the images are 500 nm \times 500 nm and the z range is 3 nm.

example, they are not an ideal platform for the study of biomaterials.

2. Homogeneous Mixed Disulfides. Figure 4 shows AFM images of the mixed SAMs formed by coadsorption of $\text{CH}_3(\text{CH}_2)_{17}\text{S}-\text{S}(\text{CH}_2)_{10}\text{CH}_2\text{OH}$ and $\text{HO}(\text{CH}_2)(\text{CH}_2)_{10}\text{S}-\text{S}(\text{CH}_2)_{10}\text{CH}_2\text{OH}$, which were immediately brought out of solutions (panels a–d) and kept in air for 3 days (panels a'–d'). Phase segregation was not observed on all cases. Some small holes

were found in the AFM images of pure asymmetric disulfide (Figure 4, panels a and a') due to the lower coverage of disulfides. Because of the lower activity of disulfides than thiols,²³ the coverage of mixed SAMs of disulfides is usually lower than that of thiols.²⁴ Our XPS results show that the C/Au ratios of the mixed SAMs of disulfides are slightly less than those of thiols when their surface compositions are equal. For the mixed SAMs of symmetric and asymmetric disulfides

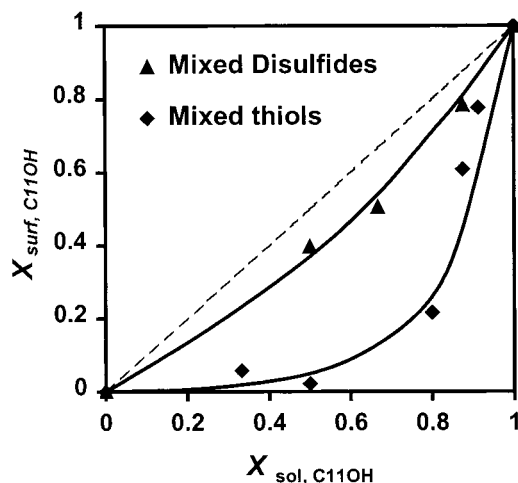


Figure 5. Comparison of surface compositions (molar fraction) between the mixed SAMs formed by thiols and disulfides. $X_{\text{sol, C11OH}}$ is the solution composition of $\text{HOCH}_2(\text{CH}_2)_{10}\text{S}-$ chain while $X_{\text{surf, C11OH}}$ is the surface composition of $\text{HOCH}_2(\text{CH}_2)_{10}\text{S}-$ chain determined from XPS by scaling the O(1s) signal of the mixed SAMs to that of the pure $\text{HOCH}_2(\text{CH}_2)_{10}\text{SH}$ SAMs. Solid lines are drawn to guide the eye.

studied in this work, solution compositions of short chains vary from 0.5 to 0.9, while surface compositions of short chain vary from 0.40 to 0.80 determined by XPS. On the contrary, the mixed SAMs of thiols with the same two kinds of chains and similar surface compositions led to phase segregation as shown in the previous section. To compare the different behaviors of thiols and disulfides, in addition to AFM and FFM, XPS experiments were also carried out. XPS results in Figure 5 show that at the same solution composition the corresponding surface composition in mixed SAMs of disulfides is close to the ideal 1:1 line where no preferential adsorption occurs and surface and solution compositions should be the same, whereas for mixed SAMs of thiols it deviates significantly from the 1:1 line. This indicates that there is less preferential adsorption (or less phase segregation) in the mixed SAMs formed from disulfides than thiols. For the mixed SAMs of symmetric and asymmetric disulfides, the lattice image can still be obtained (Figure 6) although the image is not as good as those of pure SAMs due to the large chain length difference in the mixed SAMs. The lattice constant (~ 0.5 nm) is the same as that of pure SAMs, indicating that the mixed SAMs formed from the coadsorption of symmetric and asymmetric disulfides possess highly ordered structures on Au(111). In the competitive adsorption of thiols and disulfides, the thiol was preferred by a factor of $\sim 75:1$ over the disulfide.²³ Therefore, highly purified disulfides are very important to this work. Our disulfide samples have been purified by flash chromatography and double recrystallization to avoid any effects due to the disulfide samples contaminated with thiols.

As described above, no obvious phase segregation was found on those formed from disulfides while phase segregation was found on mixed SAMs formed from thiols. The possible mechanism is as follows. The basic processes for adsorption, desorption, and assembling of disulfides on Au(111) surfaces are similar to those of alkanethiols. The thermodynamic principle governing their phase behavior is also the same. That is, the order of the stability of alkyl chain pairs in the SAMs is long chain—long chain > short chain—short chain > long chain—short chain. As illustrated in Figure 1, for the coadsorption of disulfides, when the preferential adsorption of long chain pairs occurs, each long chain moiety will bring in a short chain due to the structure of the asymmetric disulfide, which has one

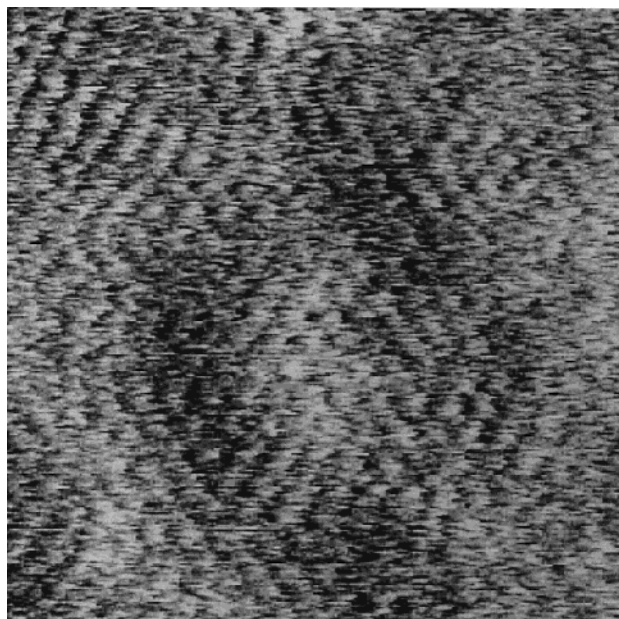


Figure 6. Frictional image of the mixed SAMs formed by asymmetric disulfides. The image has a periodicity of ~ 0.5 nm, which is the same as that of pure alkanethiols. The dimensions of the image are $10 \text{ nm} \times 10 \text{ nm}$.

long chain and one short chain covalently bound by S—S in solution. The short chains around a long chain block further aggregation of long chains, thus reducing the possibility of phase segregation. Although the S—S disulfide bond is stable in solution, once a disulfide adsorbs on the gold surface, the competing S—Au bond could result in cleavage of the S—S bond. New ab initio calculations²⁵ showed that dissociation was clearly favored for the disulfide with subsequent formation of strongly bound thiolates. Recent experiments^{14,15,26} also showed the evidence for the cleavage of disulfides in the SAMs on Au(111). After disulfides adsorb on the surface, exchange may occur between short chains on the surface and disulfides in the solution, which usually starts at the defect sites. When exchange occurs, an asymmetric disulfide molecule will always come from solution to surface with a short and a long chain through the S—S bond. Moreover, since the adsorption and diffusion rates of disulfides are slower than those of thiols, the replacement of a short chain on the surface with a disulfide molecule in solution will be slow. All of these factors combined together result in the less preferential adsorption of the long chain moiety in the coadsorption of the mixed disulfides than the mixed thiols. Hence, the SAMs formed from the mixed symmetric and asymmetric disulfides are homogeneous. The results are supported by our XPS data and AFM images.

Since dialkyl disulfides are important alternatives to alkanethiols for the formation of SAMs, several groups reported the studies of SAMs formed from different dialkyl disulfides. Among them, characterizations by XPS,²⁷ TOF—SIMS,²⁷ contact angle,²⁸ and AFM/FFM²⁹ of many SAMs formed from asymmetric dialkyl disulfides suggest no obvious deviation from 1:1 composition. Recently, Heister et al.¹⁴ reported that significant deviations from 1:1 were found based on the XPS and NEXAFS data and Noh et al.¹⁵ showed chain interchange on surface upon the dissociative adsorption of asymmetric disulfide under very low surface coverage. We consider that the main difference among these results comes from different levels of SAM defects. The compact structure of homogeneous mixed SAMs on atomically flat Au(111) used in our work enables the formation of kinetically trapped state,¹³ whereas polycrystalline gold used

by Heister et al.¹⁴ or very low surface coverage¹⁵ cannot kinetically trap mixed SAMs in the homogeneous state. The deviation from 1:1 composition was mainly caused by a significant amount of defects on polycrystalline gold and chain interchange on the surface upon the dissociative adsorption of asymmetric disulfide occurring only under very low surface coverage.

Conclusions

In this work, we observed that for SAMs produced using mixed symmetric and asymmetric disulfides on atomically flat gold, no phase segregation and less preferential adsorption occurred. However, for SAMs produced using two different thiols on gold, phase segregation and preferential adsorption occurred. The disulfides were chosen so as to produce the same surface thiolates as the thiols in this work. When the disulfides adsorb, each long chain moiety will bring in a short chain due to the structure of the asymmetric disulfide. The short chains around a long chain block further aggregation of long chains and stop forming the domains of long chains, thus reducing the possibility of phase segregation. We consider that atomically flat Au(111) surfaces used in this work are very important to the formation of kinetically trapped and compact homogeneous mixed SAMs, whereas polycrystalline gold used in some previous studies cannot kinetically trap mixed SAMs in the homogeneous state. Different results come from the fact that different gold surfaces were used. Our results suggest that the coadsorption of asymmetric and symmetric disulfides be one of the approaches to prepare homogeneous mixed SAMs at a wide range of surface compositions. As the use of mixed SAMs as a platform of biomimetic surfaces increases, both convenient methods proposed here and previously¹³ will be useful to control chemical, structural, and biological properties of surfaces.

Acknowledgment. This work is supported by the National Science Foundation (CTS-9815436 and CTS-9983895).

References and Notes

- (1) (a) Ostuni, E.; Yan, L.; Whitesides, G. M. *Colloids Surfaces B: Biointerface* **1999**, *15*, 3. (b) Mrksich, M.; Whitesides, G. M. *Annu. Rev. Biophys. Biomol. Struct.* **1996**, *25*, 55.
- (2) (a) Lestelius, M.; Liedberg, B.; Tengvall, P. *Langmuir* **1997**, *13*, 5900. (b) Kidoaki, S.; Matsuda, T. *Langmuir* **1989**, *5*, 7639.
- (3) Wink, I.; van Zuilen, S. J.; Bult, A.; van Bennekom, W. P. *Analyst* **1997**, *122*, 43R.
- (4) Valiokas, R.; Svedhem, S.; Svensson, S. C. T.; Liedberg, B. *Langmuir* **1999**, *15*, 3390.
- (5) (a) Higashi, N.; Takahashi, M.; Niwa, M. *Langmuir* **1999**, *15*, 111. (b) Lahiri, J.; Isaacs, L.; Grzybowski, B.; Carbeck, J. D.; Whitesides, G. M. *Langmuir* **1999**, *15*, 7186. (c) Patel, N.; Davies, M. C.; Heaton, R. J.; Tandler, S. J. B.; Williams, P. M. *Appl. Phys. A* **1998**, *66*, S569.
- (6) (a) Bain, C. D.; Whitesides, G. M. *J. Am. Chem. Soc.* **1989**, *111*, 7164. (b) Tamada, K.; Hara, M.; Sasabe, H.; Knoll, W. *Langmuir* **1997**, *13*, 1558.
- (7) (a) Mizutani, W.; Ishida, T.; Yamamoto, S.-I.; Tokumoto, H.; Hokari, H.; Azebara, H.; Fujihira, M. *Appl. Phys. A* **1998**, *66*, S1257. (b) Kang, J. F.; Ulman, A.; Liao, S.; Jordan, R. *Langmuir* **1999**, *15*, 2095.
- (8) Hobara, D.; Ota, M.; Imabayashi, S.-I.; Niki, K.; Kakiuchi, T. *J. Electroanal. Chem.* **1998**, *444*, 113.
- (9) (a) Delamarche, E.; Michel, B. *Thin Solid Films* **1996**, *273*, 54. (b) Delamarche, E.; Michel, B.; Biebuyck, H. A.; Gerber, C. *Adv. Mater.* **1996**, *8* (9), 719.
- (10) Allara, D. L.; Dunbar, T. D.; Weiss, P. S.; Bumm, L. A.; Cygan, M. T.; Tour, J. M.; Reinert, W. A.; Yao, Y.-T.; Kozaki, M.; Jones, L., II *Ann. N. Y. Acad. Sci.* **1998**, *852*, 349.
- (11) Ge, S.; Takahara, A.; Kajiyama, T. *Langmuir* **1995**, *11*, 1341.
- (12) (a) Pan, S.; Castner, D. V.; Ratner, B. D. *Langmuir* **1998**, *14*, 3545. (b) Bertilsson, L.; Liedberg, B. *Langmuir* **1993**, *9*, 141.
- (13) Chen, S.; Li, L.; Boozer, C. L.; Jiang, S. *Langmuir* **2000**, *16*, 9287.
- (14) Heister, K.; Allara, D. L.; Bahnck, K.; Frey, S.; Zharnikov, M.; Grunze, M. *Langmuir* **1999**, *15*, 5440.
- (15) Noh, J.; Hara, M. *Langmuir* **2000**, *16*, 2045.
- (16) Folkers, J. P.; Laibinis, P. E.; Whitesides, G. M. *Langmuir* **1992**, *8*, 1330.
- (17) Overney, R. M.; Meyer, E.; Frommer, J.; Brodbeck, D.; Luthir, R.; Howald, L.; Guntherodt, H. J.; Fujihira, M.; Takano, H.; Gotoh, Y. *Nature* **1992**, *359*, 133.
- (18) Milligan, B.; Swan, J. M. *J. Chem. Soc.* **1962**, 2172.
- (19) Li, L.; Chen, S.; Jiang, S. in *Interfacial Properties on the Submicron Scale*; Frommer, J. E.; Overney, R., Eds.; ACS Symposium Series, 2000.
- (20) (a) Porior, G. E. *Langmuir* **1999**, *15*, 1167. (b) Xu, S.; Cruchon-dupeyrat, S. J. N.; Garno, J. C.; Liu, G.-Y.; Jennings, G. K.; Yong, T.-H.; Laibinis, P. E. *J. Chem. Phys.* **1998**, *108*, 5002.
- (21) Schlenoff, J. B.; Li, M.; Ly, H. *J. Am. Chem. Soc.* **1995**, *117*, 12528.
- (22) Yamada, R.; Uosaki, K. *Langmuir* **1998**, *14*, 855. (b) Arce, F. T.; Vela, M. E.; Salvarezza, R. C.; Arvia, A. J. *Langmuir* **1998**, *14*, 7203. (c) Schonenberger, C.; Jorritsma, J.; Sondag-Huethorst, J. A. M.; Fokink, L. G. J. *J. Phys. Chem.* **1995**, *99*, 3259.
- (23) Bain, C. D.; Biebuyck, H. A.; Whitesides, G. M. *Langmuir* **1989**, *5*, 723.
- (24) Private communication with H. Schonherr, Stanford University, 1999.
- (25) Grönbeck, H.; Curioni, A.; and Andreoni, W. *J. Am. Chem. Soc.* **2000**, *122*, 3839.
- (26) Ishida, T.; Yamamoto, S.; Mizutani, W.; Motomatsu, M.; Tokumoto, H.; Hokari, H.; Azebara, H.; Fujihira, M. *Langmuir* **1997**, *25*, 33261.
- (27) (a) Biebuyck, H. A.; Whitesides, G. M.; *Langmuir* **1993**, *9*, 1766. (b) Offord, D. A.; John, M.; Griffin, J. H. *Langmuir* **1994**, *10*, 761.
- (28) Biebuyck, H. A.; Bain, C. D.; Whitesides, G. M. *Langmuir* **1994**, *10*, 1825.
- (29) Schonherr, H.; Ringsdorf, H. *Langmuir* **1996**, *12*, 3891.